مجلـــة كليـــة التربيـــة طرابلـــس

Journal of the Faculty of Education Tripoli

First-principles Density Functional Study of Nickel and Nickel-complex in Diamond

[1*]A. M. Gsiea,[2]M. K. Atumi, [3]J. P. Goss, [4]P. R. Briddon, [5]F. A. Gsiea.
[1,2] Department of Physics, Faculty of Education, University of Tripoli, Tripoli, Libya.
[3, 4] School of Electric, Electronic and Computer Engineering, Newcastle University, Newcastle upon Tyne, UK.
[5]Computer Department, College of Electronic Technology, Tripoli, Libya.
[*]Corresponding: a.gsiea@uot.edu.ly

دراسة شائبة النيكل والشوائب ذات العلاقة في الألماس باستخدام المبادئ الأولية لنظرية كثافة الدالة

Article history
Received: May 9, 2024 Accepted: May 19, 2024

الملخص:

يعتبر الماس مادة جذابة للعلماء لما له من خصائص فيزيائية و كهربائية ممتازة. يمكن استخدامه في الأجهزة البصرية لانبعاث الضوء فوق البنفسجي وفي الأجهزة الإلكترونية ذات التطبيقات الطاقة العالية و التردد العالي. نقدم دراسة شائبة النيكل في الالماس باستخدام نظرية كثافة الدالة. التركيب البلوري، معلومات الطاقة، مستويات الانتقال الالكتروني والرنين البارامغناطيسي الإلكتروني تم دراستهم لجميع الشوائب الخلالية والاستبدالية والشوائب ذات الصلة المحتملة تكوينها. توافقت حساباتنا المتحصل عليها و المستندة إلى نظرية كثافة الدالة مع تفسيرات أخرى، خاصة فيما يتعلق بالرنين المغنطيسي الإلكتروني، والطاقات الانتقالية للنيكل في الماس.

الكلمات المفتاحية: نيكل، شائبة، الماس، نظرية كثافة الدالة.

A B S T R A C T:

Diamond is an attractive material for scientists due to its excellent physical and electrical properties. It can be utilised in optical devices for ultraviolet light emission and in electronic devices for high power and high frequency applications. We present a first-principles density functional theory study of nickel impurities in diamond. The atomic structures, formation and transition energies, and hyperfine parameters of nickel interstitial, substitutional, and related defects were computed using ab initio total energy methods. Our calculations, based on local density functional theory, are in agreement with other interpretations, particularly regarding electron paramagnetic resonance, and transition energies of nickel in diamond.
Keywords: Diamond, DFT, Defects, Nickel.

Introduction:

Synthetic diamond can be grown from graphite by subjecting it to high pressure, high temperature conditions in the presence of a transition metal catalyst. The most commonly used catalysts are alloys containing manganese, iron, nickel, and cobalt [1–5]. However, the incorporation of transition metals into the resulting diamond crystal can lead to the formation of electrically active centres with absorption bands in the visible spectra. Of these transition metals, nickel has been unambiguously identified as present in synthetic diamond by various experimental techniques such as electron paramagnetic resonance (EPR) and optical absorption measurements. Active centres related to isolated nickel [4, 5], and nickel-related complexes involving intrinsic defects or dopants [6] have been identified using these techniques. However, there is still debate and controversy regarding the exact microscopic structure of these centres.

Using EPR [4] and optical measurements [7], isolated nickel in diamond has been shown to exhibit tetrahedral symmetry and possess a spin of 3/2.

The W8 centre, designated as such, is believed to be created by a solitary substitutional nickel in the negative charge state (Ni_s^{-1}) with a $3d^7$ configuration [4]. Further EPR investigations led to the discovery of two other significant active diamond centres, namely NIRIM-1 and NIRIM-2 [5]. At low temperatures ($T \leq 25$ K), the NIRIM-1 centre was identified to have a spin of 1/2 and exhibit trigonal symmetry, while at higher temperatures it displayed tetrahedral symmetry. One interpretation suggests that this centre arises from a single nickel interstitial in the positive charge state (Ni_i^{+1}) with a $3d^9$ configuration. The NIRIM-2 centre, with a spin of 1/2 and trigonal symmetry, has been observed through EPR [5] and optical [8,9] observations.

Several microscopic models have been proposed for this centre, including the possibility of an interstitial nickel in a strong trigonal field induced by a neighbouring vacancy or impurity, which is consistent with the observed g values of (g=2.32 and g =0) [5].

Method:

Density functional theory, which is implemented in AIMPRO package [10,11], has been used in this study. Defects are simulated by employing large super-cells and periodic boundary conditions. The cells consist of repeated primitive face-centred cubic (fcc) unit cells containing eight carbon atoms. We have analysed Ni-centres in supercells composed of 64 atoms, composed from (2 × 2 × 2) primitive cells.

The Brillouin zone is sampled using the Monkhorst-Pack scheme [12], typically with a mesh of (2 × 2 × 2) k-points. The structures are optimised using a conjugate-gradient scheme until the energy change between iterations is less than 10^{-5} Ha.

Atoms are simulated using ab initio pseudopotentials [13], and the total energies and forces are obtained using a local density approximation for the exchange-correlation [14]. The wave functions and charge density are expanded in terms of Gaussian orbitals and plane waves, respectively [15].

For carbon (C) and nickel (Ni), we include s, p and d functions, resulting in a total of 28 and 32 functions per atom, respectively. Plane waves up to 150 Ha are used to expand the charge density.

We calculate the formation energy of a defect X using the equation:

$$E^f(X, q) = E^{tot}(X, q) - \mu_i + q\mu_e + \zeta(X, q) \qquad (1)$$

where $E^{tot}(X, q)$ is the total energy calculated for the system X containing the defect in charge state q. μ_i represents the chemical potential of species (i =C and Ni). $E_v(X, q)$ is the Fermi energy at the valance-band top, and μe is the electron chemical potential, which is defined as zero at the valence-band top.

The chemical potential for Ni is taken as that of the Ni metal.

To study the electrical characteristics of the defect centres, we calculate the transition levels, E(q, q′), which are defined as the electron chemical potentials at which the formation

energies for two charge states, q and q′, are equal. For example, the donor level is the value of μe for which E^f (X, 0) = E^f (X, +1), and E^f (X, 0) = E^f (X, −1) for the acceptor level.
Both the lattice constant and bulk modulus of pure diamond have been calculated using diamond-pdpp basis sets. The total energy was obtained as a function of volume, and the Burch-Murnighan equation of state was used for fitting. The results of electronic properties of diamond, such as the lattice constant, bulk modulus, and energy band gap, are as follows: a=3.53Å, B=4.42 Mbar, and Eg=4.5 (eV). These values are very close to the experimental calculation a=3.567Å, B=4.42Mbar and Eg=5.48(eV) [16].

Result and Discussion

First, we examine a diamond with a nickel impurity substitution. Examination of the relaxed structure, shown schematically in (Fig 1), indicates that the nickel atom remains on-site and exhibits tetrahedral symmetry with four neighbouring carbon atoms.
The distance between Ni_s^0 and its first four carbon neighbours is 1.75Å, moving outward by 0.22Å, in excellent agreement with previous calculations [17–19]. The distance between Ni_s^0 and its second neighbour carbon atoms (NN) is 2.53Å, while it is 2.50Å for C-C bond of pure diamond.

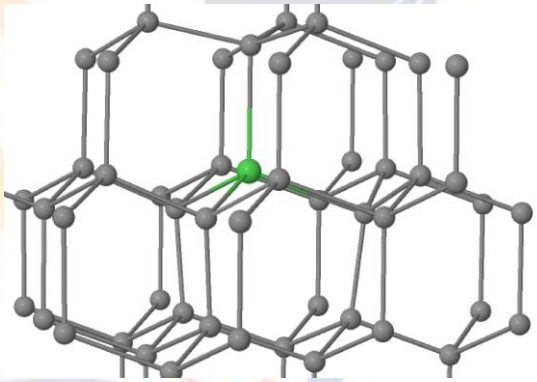

Fig. 1: Schematic structures of Nis.

However, for the neutral charge state of Ni_s^0, the total energy of the spin S=1 is higher than spin S=0 by about 0.13 eV, where they have T_d symmetry.

The electrical levels of Ni_s have been estimated by calculating the formation energy as a function of charge state and μ_e using the relationship 1. The charge-dependent formation energies yield both donor and acceptor levels in the band-gap, which are summarised in (Fig 3). The donor levels are calculated at around E_v+1.6 eV and E_v+0.7 eV for (0/+) and (+1/+2) transitions, respectively.

The acceptor transition energy (0/-) of the Ni_s^{-1} is E_v+2.98 eV where E_v defines the valance band top. This value is in excellent agreement with the experimental value of E_v+3.0 eV [20, 21], and theoretical value of E_v+2.9 eV [18]. Further note that the absorption line 2.51 eV [22–24], photoluminescence (PL) at 2.56 eV [25, 26], and optically detected magnetic resonance (ODMR) [25, 26] centres are associated with the W8 EPR centre.

The negative substitutional nickel centre (Ni_s^{-1}) has a T_d symmetry as well and presents an effective spin S=3/2 [27–32].

We have also examined the possibility for Ni_s to form pairs. One may expect a strong Coulomb attractive between these centres. There are many possible Ni_sNi_s orientations determined by the carbon positions relative to Nis, all of which are at least metastable. The most stable structure is shown in (Fig 2) which has C_{3v} symmetry.

The energies of the various orientations where the Ni_s are in the nearest shell of carbon to the Ni_s, and indeed by increasing the distance between two Ni_s in the same simulation cell, the energy increases by (1.06) eV. It is more realistic to describe the system not as $2Ni_s$ but as Ni_sVcNi_i

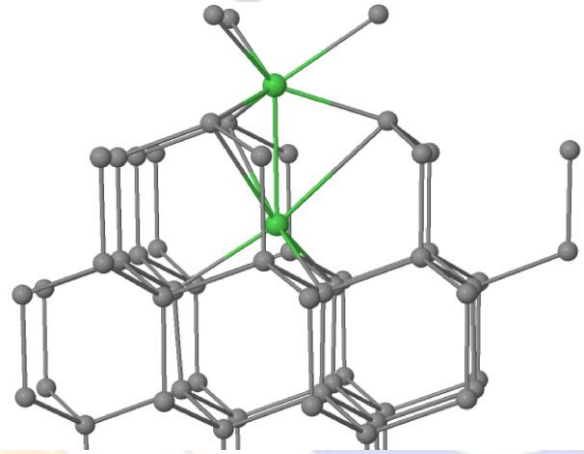

Fig. 2: Schematic structures of $2Ni_s$

.

By calculating the formation energy as a function of the charge state and μe, the electrical levels of 2Nis can be estimated. The results are shown in (Fig 3).

We find that $2Ni_s$ is thermodynamically stable as a Ni_s charge state with different level positions. The donor levels are calculated to be around E_v+1.22 eV and E_v+0.7 eV for (0/+) and (+1/+2) transitions, respectively.

The acceptor transition energies (0/-1) and (-1/-2) of the ($2Ni_s$) are E_v+1.96 eV and E_v+2.39eV, where E_v defines the valence band top. The values of the transition level E_v+1.22eV, and Ev+1.96eV are in excellent agreement with the experimental value of E_v+1.22 eV, and E_v+1.93 eV [33–35].

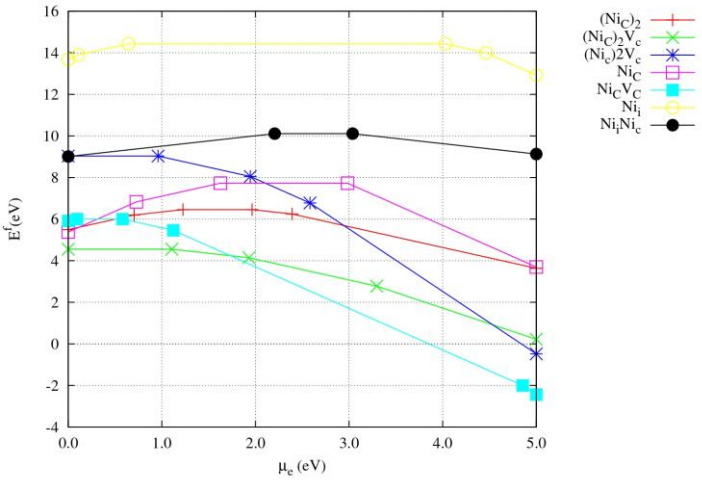

Fig. 3: Plot of E^f vs. μ_e for Ni-containing defects in diamond calculated using the 64 atoms supercell with different charge state

Although Ni_s is a donor-acceptor pair, it can be converted into an acceptor by forming a complex with a vacancy.

This is possible because Vc has a -4 charge state, and the stability of the complex will be favourably influenced by the attractive Coulomb interaction. There are many possible Ni_sV_C orientations determined by the V_C positions relative to Ni_s, all of which return to the seam structure where the vacancies are in the nearest shell of Nis, as illustrated in (Fig 4).

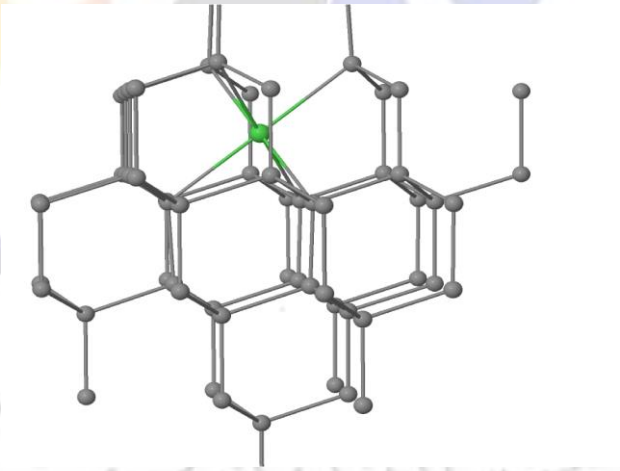

Fig. 4: Schematic structures of NiCVC.

When Ni_s is bonded with six neighbouring carbon atoms, it produces two empty states and one filled state, as shown in (Fig 3). The acceptor transition energies (0/-1) and (-1/-2) of the Ni_sVC are E_v+0.58 eV, E_v+1.12 eV, respectively, and the donor transition energy (1/0) is Ev+0.11 eV, where Ev defines the valence band top.

The possibility of nickel lying in an interstitial site (Ni_i) has been examined. Since it is found that such defects spontaneously react with the carbon in the lattice, there are a number of metastable Ni_i structures, separated by differences in total energy but chemically

distinct with different numbers and orientations of Ni-C and C-C bonds. The most stable structure we found is illustrated in (Fig 5), where it has C1 symmetry.

With respect to the final structure of the nickel interstitial, the nickel impurity distance is 1.76Å from one of its nearest neighbours while others are 1.70Å from its other three nearest neighbours. Fig 3 shows a plot including the formation energies of Ni_i in diamond.

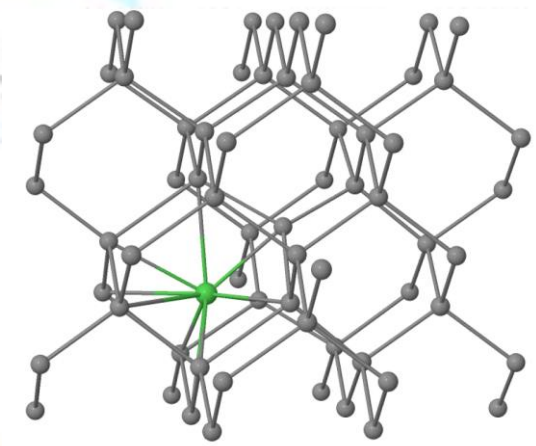

Fig. 5: Schematic structures of (Ni)i.

This yields deep donor and acceptor levels in the band-gap. We discovered that the nickel interstitial centre's formation energy is 8.7eV higher than the nickel substitutional centres, which is close to the other theoretical calculation [36].

As a result, substitutional nickel is significantly more stable than interstitial nickel in terms of total energy. However when relaxed interstitial Nickel with the first neighbour vacancy the nickel atom emigrates to the vacancy and becomes substituting. According to the low energy barrier of interstitial nickel in diamonds [37], it will not exist alone especially at high temperatures.

However, nickel interstitials could be formed with other defects as a nickel pair or with di-vacancy. Based upon the formation energies, there are a deep acceptor calculated at around E_v+4.23eV and E_v+4.66eV for (0/-) and (-1/-2) transitions, respectively. The donor levels are calculated at around E_v+0.84eV and E_v+0.31eV for (0/+) and (+1/+2) transitions, respectively.

Nickel interstitial diamond is thermodynamically stable in neutral, positive, and negative charge states, according to data on the formation energy and band structure. Combining the formation energy data strongly suggests that nickel substitutional diamond is thermodynamically stable at neutral, positive and negative charge states.

Tab. 1: Calculated symmetry, spin, transition energies and hyperfine parameters (A) in MHz, in the Ni^{61} nucleus.

Defects	Symm.	Spin	Et(eV)	Hyperfine		
				A_1	A_1	A_1
Ni_S^{+2}	C_{3V}	0	0.7(1/2)	.	.	.
Ni_S^{+1}	C_{3V}	1/2	1.6 (0/+)	23.34	23.34	23.34
Ni_S^{-1}	T_d	3/2	2.98(-1/0)	20.06	20.06	20.06
Ni_S^{-2}	T_d	1	0.76(-2/-1)	21.96	21.96	21.96
Ni_i^{+1}	C_{2S}	1/2	0.64 (0/+)	6.87	7.52	13.75
Ni_i^{-1}	C_{2S}	1/2	4.03(-1/0)	10.64	10.66	15.45
$Ni_S V_C^{o}$	C_{3V}	1	.	17.04	17.04	18.90
$Ni_S V_C^{+1}$	C_{3V}	1/2	0.11(0/1)	18.2	18.2	20.7
$Ni_S V_C^{-1}$	C_{3V}	1/2	0.58(-1/0)	16.48	16.48	18.21
$Ni_S V_C^{-2}$	C_{3V}	0	1.12(-2/-1)	.	.	.
$Ni_S 2V_C^{-1}$	C_{2S}	1/2	0.96(-1/0)	18.08	13.26	12.53
$Ni_S 2V_C^{-2}$	C_{2S}	0	1.94(-2/-1)	.	.	.
$Ni_S 2V_C^{-3}$	C_{2S}	1/2	2.58(-3/-2)	20.69	43.13	85.35
$2Ni_S^{0}$	C_{3V}	1	.	1.92	1.92	3.30
$2Ni_S^{+1}$	C_{3V}	1/2	1.22 (0/+)	34.06 1.04	8.29 1.04	8.29 3.73
$2Ni_S^{+2}$	C_{3V}	0	0.7(+1/+2)	.	.	.
$2Ni_S^{-1}$	C_{3V}	1/2	1.96(-1/0)	32.63 3.08	9.89 3.08	9.89 4.23
$2Ni_S^{-2}$	C_{3V}	0	2.39(-2/-1)	.	.	.
$2Ni_S V_C^{-1}$	C_{2V}	1/2	1.11(-1/0)	37.39 2.36	23.18 3.32	17.22 16.17
$2Ni_S V_C^{-2}$	C_{2V}	0	1.93(-2/-1)	.	.	.
$2Ni_S V_C^{-3}$	C_{2V}	1/2	3.30(-3/-2)	27.65 27.65	25.67 25.67	39.65 39.65
$Ni_S Ni_i^{+1}$	C_{3V}	1/2	2.21 (0/+)	378.5 44.70	335.08 38.75	335.08 38.75
$Ni_S Ni_i^{-1}$	C_{3V}	1/2	3.04(-1/0)	51.19 2.64	51.19 5.18	41.86 5.18

Table 1 shows the symmetry, spin, transition energies, and hyperfine parameters calculated for all the nickel centres and related defects in diamond. The hyperfine interactions between the unpaired electron and the nucleus of C^{13} in the defect are modelled [38].

Conclusion:

The study provides a comprehensive overview of the properties of nickel impurities in diamond, including their structure, energy levels, stability, and interactions with other defects. They also introduce a table that summarises these properties for various nickel centres and related defects. Depending on the position of the Fermi level in diamond, the $2Ni_SV$, Ni_SV, and $2Ni_S$ defects are the most stable forms of nickel impurity in diamond, respectively. We suggest that the $2Ni_SV$, Ni_SV, and $2Ni_S$ structures are related to the optical (EPR) centres in diamond as 1.22 eV (NOL1/NIRIM-5) could be related to $2Ni_S^{+1}$ and Ni_SV^{-2}, 1.93 eV (NIRIM-2), related to $2Ni_SV^{-2}$, $2Ni_S^{-1}$ and Ni_S2V^{-1}, and 2.964 eV related to Ni_S^{-1}.

References:

[1] J. C. Angus, and C. C. Hayman, Science. 214, 913 (1988).

[2] G. Davies, A. J. Neves, and M. H. Nazare, Europhys Lett. 9, 47 (1989).

[3] D. J. Twitchen, J. M. Baker, M. E. Newton, and K.Johnston, Phys. Rev. B 61, 9 (2000).

[4] J. Isoya, H. Kanda, J. R. Norris, J. Tang, and M. K. Bowman, Phys. Rev. B 41, 3905 (1990).

[5] J. Isoya, H. Kanda, and Y. Uchida, Phys. Rev. B 42, 9843 (1990).

[6] V. A. Nadolinny, A. P. Yelisseyev, J. M. Baker, M. E. Newton, D. J. Twitchen, S. C. Lawson, O. P. yuryeva, and B. N. Feigelson, J. Phys. Condens. Matter 11, 7357 (1999).

[7] M. H. Nazare, J. C. Lopes, and A. J. Neves, Physica B 308-310, 616 (2001).

[8] M. H. Nazare, A. J. Neves, and G. Davies Phys. Rev. B 43, 14196 (1991).

[9] P. W. Mason, F. S. Ham, and G. D. Watkins, Phys. Rev. B 49, 5417 (1999).

[10] P. R. Briddon and R. Jones, Phys. Status Solidi B 217, 131 (2000). [11] M. J. Rayson and P. R. Briddon, Computer Phys. Comm. 178, 128 (2008).

[12] H. J. Monkhorst and J. D. Pack, Phys. Rev. B 13, 5188 (1976).

[13] N. Troullier and J. L. Martins, Phys. Rev. B 43, 1993 (1991).

[14] J. P. Perdew and Y. Wang, Phys. Rev. B 45, 13244 (1992).

[15] J. P. Goss, M. J. Shaw, and P. R. Briddon, Topics in Appl. Phys. 104, 69 (2007).

[16] Landolt-B¨Ornstein, Numerical Data and Functional Relation- ships in Science and Technology, vol. 17, edited by O. Madelung, M. Schulz, and H. Weiss (Springer-Verlag, New York, 1982).

[17] R. Larico, L. V. C. Assali, W. V. M. Machado, and J. F. Justo, Compu. Mater. Sci. 30, 62-66 (2004).

[18] R. Larico, J. F. Justo, W. V. M. Machado, and L. V. C. Assali, Brazilian Journal of Physics 34, 669 (2004).

[19] Kenji. Tsuruta, Satoshi. Emoto, Chieko. Totsuji, and Hiroo. Totsuji, Computational Material Science 38, 873-882 (2007).

[20] D. M. Hofmann, P. Christmann, D. Volm, K. Pressl, L. Pereira, L. Santos, and E.Pereira, Mater Sci. Forum 79, 196-201 (1995).

[21] D. M. Hofmann, M. Ludwing, P. Christmann, D. Volm, B. K. Meyer, L. Pereira, L. Santos, and E.Pereira, Phys. Rev. B 50, 17618 (1994).

[22] A. T. Collins, H. Kanda, J. Isoya, C. Ammerlaan, and J. van Wyk, Correlation between optical absorption and EPR in high-pressure diamond grown from a nickel solvent catalyst, Diam. Relat. Mater. 7, 333 (1998).

[23] M. H. Nazar´e, J. C. Lopes, and H. Kanda, Nickel related absorption lines in high-pressure synthetic diamond, MRS Proc. 339, 625 (1994).

[24] M. Nazar´e, J. Lopes, and A. Neves, Nickel related defects in diamond: The 2.51 eV band, Physica B (Amsterdam) 616, 308-310 (2001)

[25] E. Pereira, L. Santos, L. Pereira, D. Hofmann, P. Christmann, W. Stadler, and B. Meyer, Slow emission of the 2.56 eV centre in synthetic diamond, Diam. Relat. Mater. 4, 53 (1994).

[26] M. H. Nazare, P. W. Mason, G. D. Watkins, and H. Kanda, Optical detection of magnetic resonance of nitrogen and nickel in high-pressure synthetic diamond, Phys. Rev. B 51, 16741 (1995).

[27] J. E. Lowther, Phys. Rev. B 51, 91 (1995).

[28] R. Larico, J. Justo, W. Machado, and L. Assali, An ab initio investigation on nickel impurities in diamond, Phys. B (Amsterdam) 84, 340-342 (2003)

[29] R. Larico, L. V. C. Assali, W. V. M. Machado, and J. F. Justo, Isolated nickel impurities in diamond: A microscopic model for the electrically active centres, Appl. Phys. Lett. 84, 720 (2004).

[30] R. Larico, L. Assali, W. Machado, and J. Justo, Nickel impurities in diamond: a FP-LAPW investigation, Comput. Mater. Sci. 30, 62 (2004).

[31] R. Larico, L. V. C. Assali, W. V. M. Machado, and J. F. Justo, Erratum: isolated nickel impurities in diamond: A microscopic model for the electrically active centres, Appl. Phys. Lett. 85, 6293 (2004).

[32] T. Chanier and A. Gali, Ab initio characterization of a Ni-related defect in diamond: The W8 centre, Phys. Rev. B 87, 245206 (2013).

[33] E. Londero, E. Bourgeois, M. Nesladek, and A. Gali, Phys. Rev. B 97, 241202 (2018)

[34] K. Iakoubovskii, Phys. Rev. B 70, 205211 (2004)

[35] S. C. Lawson, H. Kanda, and M. Sekita, Philos. Mag. B 68, 39-46 (1993)

[36] R. Larico, J. F. Justo, W. V. M. Machado, and L. V. C. Assali, Electronic properties and hyperfine fields of nickel-related complexes in diamond, Phys. Rev. B 79, 115202 (2009).

[37] J. P. Goss, P. R. Briddon, R. Jones, and S. ¨Oberg, The lattice location of Ni in diamond: A theoretical study, J. Phys.: Condens. Matter 16, 4567 (2004).

[38] M.K. Atumi, J.P. Goss, P.R. Briddon, A.M. Gsiea, and M.J. Rayson, Result in Physics 16, 102860 (2020).